

Zeitschrift: IABSE congress report = Rapport du congrès AIPC = IVBH
Kongressbericht

Band: 8 (1968)

Rubrik: Vc. Dynamic behaviour of reinforced and prestressed concrete
buildings under horizontal forces and the design of joints (incl. wind,
earthquake, blast effects)

Nutzungsbedingungen

Die ETH-Bibliothek ist die Anbieterin der digitalisierten Zeitschriften auf E-Periodica. Sie besitzt keine Urheberrechte an den Zeitschriften und ist nicht verantwortlich für deren Inhalte. Die Rechte liegen in der Regel bei den Herausgebern beziehungsweise den externen Rechteinhabern. Das Veröffentlichen von Bildern in Print- und Online-Publikationen sowie auf Social Media-Kanälen oder Webseiten ist nur mit vorheriger Genehmigung der Rechteinhaber erlaubt. [Mehr erfahren](#)

Conditions d'utilisation

L'ETH Library est le fournisseur des revues numérisées. Elle ne détient aucun droit d'auteur sur les revues et n'est pas responsable de leur contenu. En règle générale, les droits sont détenus par les éditeurs ou les détenteurs de droits externes. La reproduction d'images dans des publications imprimées ou en ligne ainsi que sur des canaux de médias sociaux ou des sites web n'est autorisée qu'avec l'accord préalable des détenteurs des droits. [En savoir plus](#)

Terms of use

The ETH Library is the provider of the digitised journals. It does not own any copyrights to the journals and is not responsible for their content. The rights usually lie with the publishers or the external rights holders. Publishing images in print and online publications, as well as on social media channels or websites, is only permitted with the prior consent of the rights holders. [Find out more](#)

Download PDF: 30.03.2026

ETH-Bibliothek Zürich, E-Periodica, <https://www.e-periodica.ch>

V c

Comportement dynamique des bâtiments de grande hauteur, en béton armé ou en béton précontraint, soumis à des efforts horizontaux (vent, séismes, explosions). Conception des joints

Dynamisches Verhalten von bewehrten und vorgespannten Beton-Hochhäusern unter horizontalen Kräften (einschließlich Wind-, Erdbeben- und Explosionskräfte) und zweckentsprechende Ausbildung der Verbindungen

Dynamic Behaviour of Reinforced and Prestressed Concrete Buildings under Horizontal Forces and the Design of Joints (Incl. Wind, Earthquake, Blast Effects)

Leere Seite
Blank page
Page vide

DISCUSSION PRÉPARÉE / VORBEREITETE DISKUSSION / PREPARED DISCUSSION

Earthquake Response Analysis of a Reinforced Concrete Building having Four Box Columns

Analyse de la réponse aux séismes d'un bâtiment en béton armé avec quatre poteaux en caissons

Berechnung der Erdbebenreaktion eines Stahlbetongebäudes mit vier Kastensäulen

TSUKASA AOYAGI

HIDEYUKI TADA

Eng.D., Struc.Engrs.

Nikken Sekkei Komu Co., Ltd.

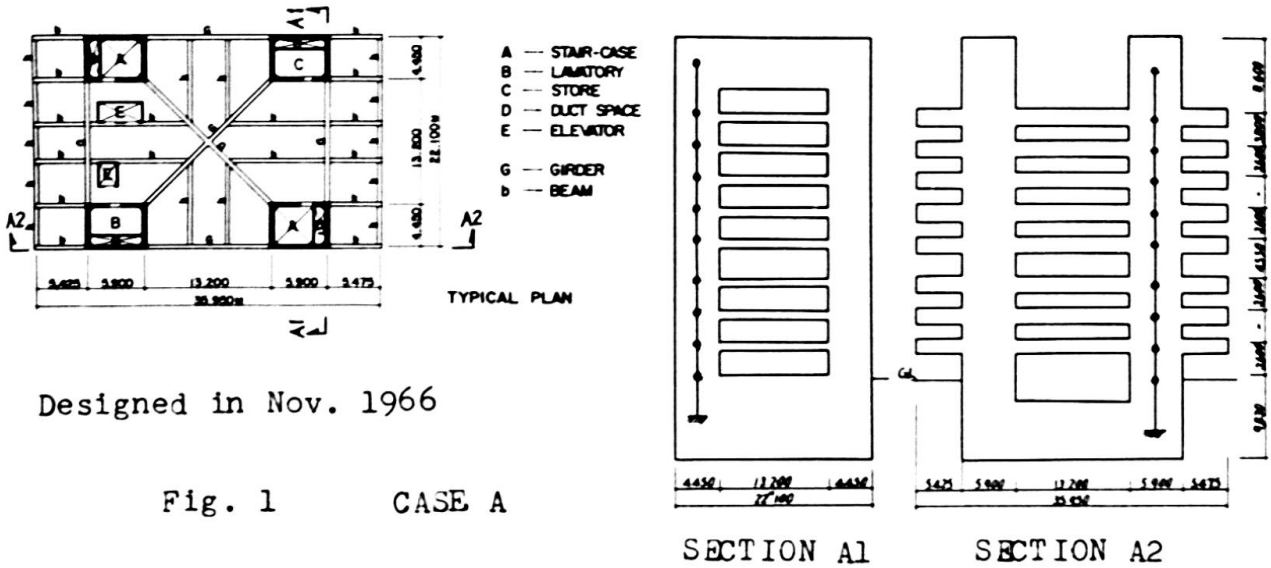
Japan

In an attempt to ascertain the earthquake response characteristics of medium-rise (30 to 45 meters in height) reinforced concrete buildings having shear walls, the authors have made analytical studies on a number of buildings of the type described above. The building (shown in Fig. 1), whose response characteristics are discussed in this paper, represents such buildings.

It is a common practice in Japan that the analysis of external vibrational force as well as the structural design of buildings is based on the loads prescribed in the national building code. Then, the structural response to the external vibrational force is analyzed to verify the appropriateness of the design. Methods of analysing such a structural response have been remarkably improved in these past years. Among them, non-linear earthquake response analysis of bending-shear type mass system seems to be favorably accepted by the increasing number of structural engineers in Japan recently.

It, however, is important for practising engineers that they should have some means to make fairly accurate assessment of a building's response to vibrational forces at the preliminary design stage so that a rational design will result thereby insuring a reasonably earthquake-resistant structure.

In this paper, an attempt will be made to deduce some earthquake response characteristics of the buildings of the type previously described from a variety of response analyses conducted by the authors while they were designing the building shown in Fig. 1. It is hoped that the results of such analyses may serve in future as a source of some useful information for preliminary structural design of similar buildings.



Designed in Nov. 1966

Fig. 1 CASE A

1. Earthquake Motions and Method of Analysis.

a. Earthquake Motions used in the Analysis.

As shown in Table 1, two ground motions, which were selected from among a number of typical earthquake motions recorded in Japan, were used for the purpose of this analysis. Of these two, the ground motion recorded in Akita represented typical earthquake motion in the soft ground while that recorded in Sendai represented one in the hard ground. Further, the N-S component of El Centro earthquake which is often used for this sort of analysis was also included so as to make possible a comparative study.

As indicated in the table, the maximum acceleration of these earthquakes were all different from one another; therefore, they were converted into the motions having a maximum acceleration of 100 gals. Fig. 2 shows the spectrum of each earthquake motion used for the analysis.

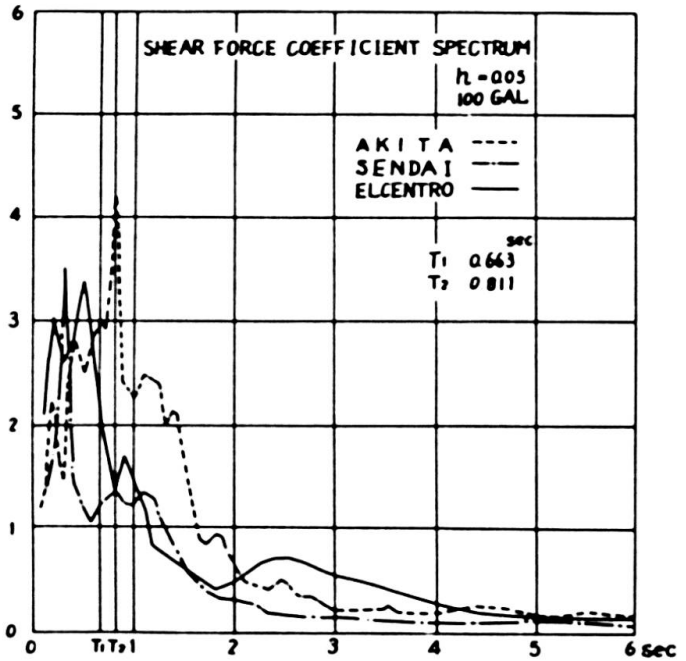


Fig. 2 LINEAR RESPONSE SPECTRUM OF ONE MASS SYSTEM

Table 1

Earthquake Names	Date	Max. Accel.	Symbols
Akita 502 NS	Jun.16 '64	90 gals	- - - - -
Sendai 501 EW	Apr.30 '62	45 gals	· · · · ·
El Centro Calif. NS	May 18 '40	319 gals	— — — —

b. Method of Analysis.Response Analysis for Bending-Shear Type Vibrational System.

For the purpose of making a non-linear earthquake response analysis of bending-shear type multi-mass point system, the following differential equation was used.

$$m_i \ddot{y}_i + \sum_{j=1}^n (1 + r_1 \frac{d}{dt}) K_{ij} \cdot y_i = -m_i \ddot{y}_0$$

where, m_i : mass at the mass point i

y_i : displacement of mass point i relative to the ground in cm

r_1 : coefficient of internal friction

k_{ij} : elastic coefficient matrix (the reaction which occurs in the direction of vibratory motion at mass point i when a unit elastic deflection is caused at point j)

\ddot{y}_0 : acceleration of ground motion

The modes (the first to the fourth) were computed by the above formula, and the responses at a specific time were amalgamated. To do this, the responses at various given times were computed by means of numerical integration using Runge-Kutta's approximation formula. For damping coefficient (h_n), the value $h_1=0.05$ was used, and it was related to frequency (ω_n) as follows:

$$h_n/\omega_n = r_1/2 = \text{constant}$$

where, n = number of modes

Response Analysis for Shear-Type Vibrational System.

The linear earthquake response analysis for shear-type multi-mass point system was made by the use of the following differential equation.

$$m_i \ddot{y}_i + (1 + r_1 \frac{d}{dt}) \{ K_i (y_i - y_{i-1}) + K_{i+1} (y_i - y_{i+1}) \} = -m_i \ddot{y}_0$$

where, m_i : mass at the mass point i

y_i : displacement of mass point i relative to the ground in cm

r_1 : coefficient of internal friction

k_i : spring constant of story i

\ddot{y}_0 : acceleration of ground motion

The values of responses were computed by applying a series of numerical integrations to this differential equation by using linear acceleration method. Further, the damping coefficient was determined based on the same assumption as used for bending-shear type system previously discussed. As for the spring constant, the value as computed on the basis of design lateral loads was used.

Table 2 Natural Periods for 1st Mode to 4th Mode

	1st	2nd	3rd	4th
direction A1	0.663	0.147	0.069	0.043
direction A2	0.811	0.173	0.073	0.043

2. Response Analysis

The building now being discussed was of simple framing design which gave no particular problem for its structural studies. In view of this, it was decided to have each story of the building represented by one mass point in both A₁ and A₂ directions by the use of the slope-deflection method in which deformation due to shear and axial force as well as rigid zone are taken into consideration, and the elastic coefficient matrix was computed accordingly. Then, the linear response analysis of bending-shear type vibrational system was conducted.

The periods are as shown in Table 2, and the excitation functions for Frame A₁ and Frame A₂ are as shown in Fig. 3 and Fig. 4 respectively.

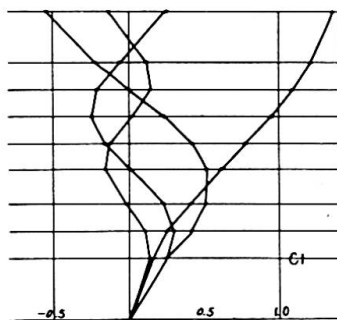


Fig. 3

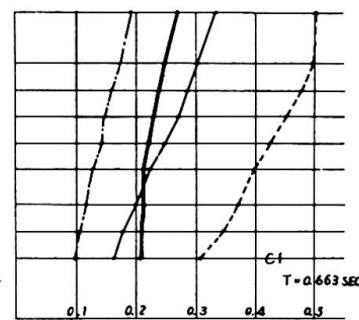


Fig. 5

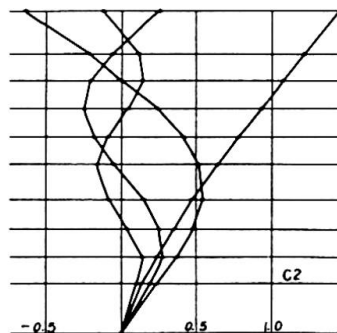


Fig. 4

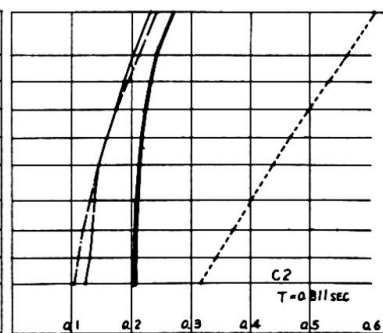


Fig. 6

AKITA -----
 SENDAI -----
 EL CENTRO -----

The response values were expressed as shear force coefficient or by symbol Q_f. These are shown in Fig. 5 and Fig. 6 for Frame A₁ and Frame A₂ respectively. (The term "shear force coefficient" as used here denotes the shear force acting on the i-th story divided by the summation of individual weight from the top down to the i-th story in question.) In Fig. 5 and Fig. 6, the shear force coefficient corresponding to the lateral loads adopted for the design of this building are shown in bold lines.

Considerations

Actually, the building now being discussed stands on a con-

tinuous layer of firm sandy gravelly soil; therefore, its behaviour under an earthquake will be assessed on the basis of response values computed for the ground motions recorded in Sendai (or El Centro). Figs. 5 and 6 indicates the response values corresponding with the maximum acceleration of ground motion which was taken as 100 gals. From these figures, it can be known that at the base of the building, the response to the acceleration of ground motion of 200 gals corresponds with the design lateral loads set out in the code; and at the top of the building, the response to the acceleration of 150 gals corresponds with the design lateral loads actually used for this building. Buildings of this type have, as shown by the studies in the past, a general tendency to give fairly larger earthquake response values at the top than at the bottom when considered in relation with the distribution of design lateral loads in the structure, so this phenomenon should be duly taken into account by the structural designer.

3. Evaluating the Method of Analysis.

Under strong earthquake motions with acceleration of 200 gals or over, most of structural members usually enter the plastic range as was the case with this building. It, therefore, is necessary to make non-linear response analysis of bending shear type vibrational system if the structural response characteristics under very severe earthquakes are to be assessed with high accuracy. Such an analysis, however, is too complicated and time-consuming for practising engineers to make in the course of actual design for which both labor and time are almost always restricted. For this reason, engineers in practice usually proceed with the structural response from linear response with the aid of the research accomplishments in the past. Since quite a variety of linear analysis methods, some intended for precise computation and others for approximation, are now available, an attempt will be made here to evaluate some of these methods on a comparative basis by applying them to the structural problems of the subject building, and on the basis of such an evaluation, some adequate method for approximate analysis that may prove a handy tool for preliminary structural design will be proposed.

For the purpose of the present comparative appraisal, the following methods of analysis will be discussed.

For precise analysis: Response analysis of the 1st to the 4th mode of bending-shear type vibrational system (expressed by symbol BS)

For approximate analysis:

- (1) Response analysis of shear type system (expressed by Symbol S)
- (2) Response analysis of the 1st mode only of bending-shear type system (expressed by Symbol BS 1st)
- (3) Response analysis of the 1st mode only to be computed from design lateral loads (expressed by Symbol S 1st), which is the method proposed by the authors.

a) Comparison of Factors in Bending-Shear Type System with Those in Shear Type System.

The difference in modes of these two systems are shown in

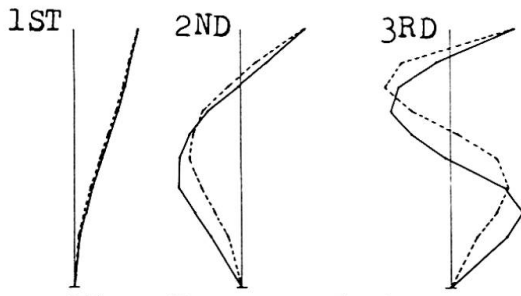


Fig. 7 Mode at Sec. A1

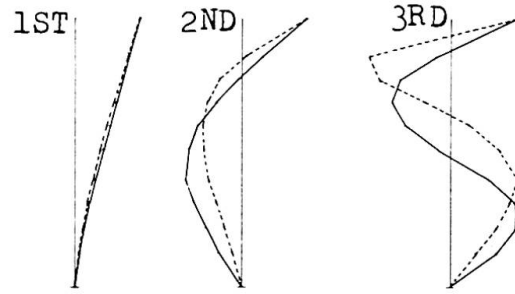


Fig. 8 Mode at Sec. A2

BS ———
S - - - - -

Fig. 7 and Fig. 8 for Frame A1 and Frame A2 respectively. Natural periods and damping coefficients for the 1st to the 4th mode are indicated in Fig. 9. These diagrams indicate that there existed a large difference between the values for bending-shear type system and those for shear type system as to all factors that were analyzed, especially at the modes of higher order. It is believed that this substantial difference is due largely to the deformation of shear walls caused by bending, which gave greater influence in the vibrational modes of higher order.

b) Comparison of Response Values (Shear Force Coefficient).

To begin with, the results obtained by analysis of the 1st mode of bending-shear type system and those of shear type system will be studied. As shown in Fig. 10, no substantial difference was observed in the analysis results of these two systems. This is only too natural because the modes of these two systems were fairly alike as can be known from Fig. 7 and Fig. 8. The results of analyses (BS) 1st/BS and S/BS are shown in Fig. 11.

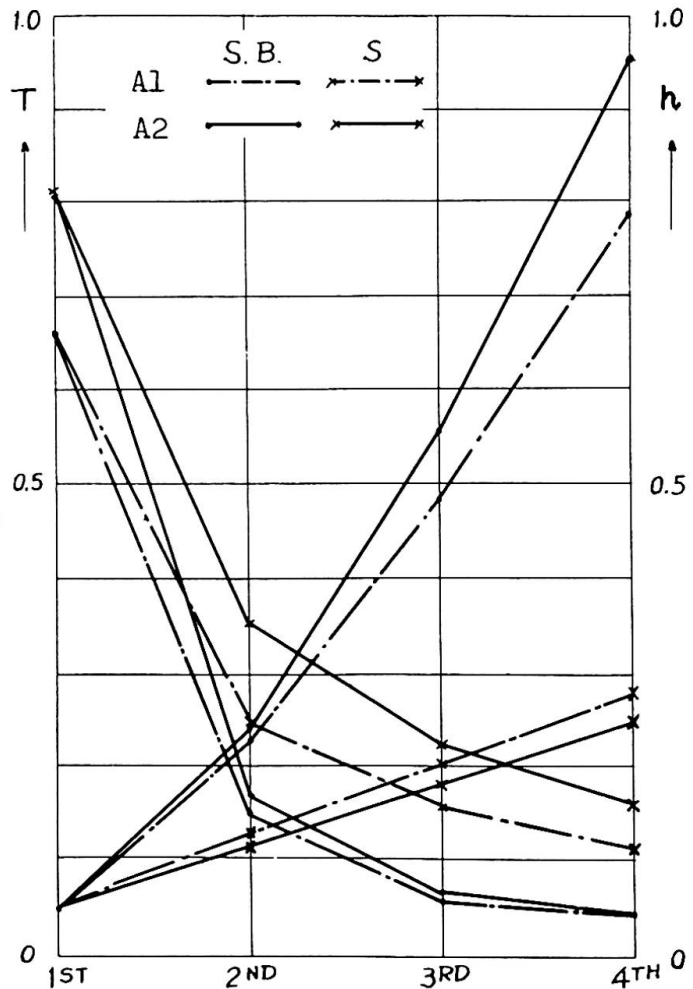


Fig. 9

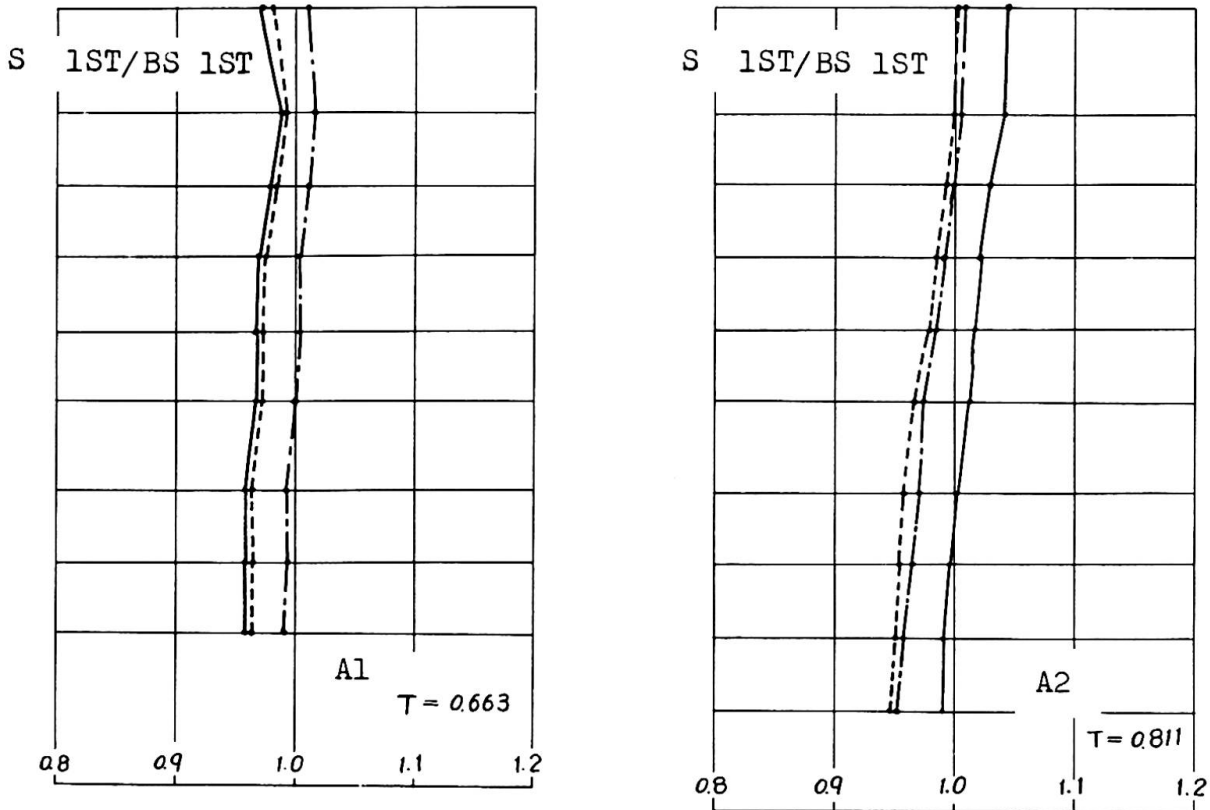


Fig. 10

AKITA -----
 SENDAI - · - · - ·
 EL CENTRO _____

Considerations.

For the purpose of these analyses, the damping coefficient, h , was determined on the assumption that there existed a relation $h_n/\omega_n = \text{constant}$. Because of this assumption, rather high damping coefficients resulted for the mode of high order in case of the bending-shear type system, and this in turn led to the response values which were little affected by the modes of high order. Thus, the response values for the 1st mode turned out to be only slightly different from those for the modes of higher orders.

In the analysis of the shear type system, however, the effects of different vibration modes (Figs. 7 and 8) gave significant effects on the response values (see Fig. 9), and thus some complicated difference was observed due to the variation of modes.

An approximate method of analysis should always be used with caution especially when such a method is intended to deduce the structural response to all types of vibrational modes from only one mode of lower degree, because in some buildings (for instance a building in Example B), their structural responses will be greatly affected by the modes of higher orders.

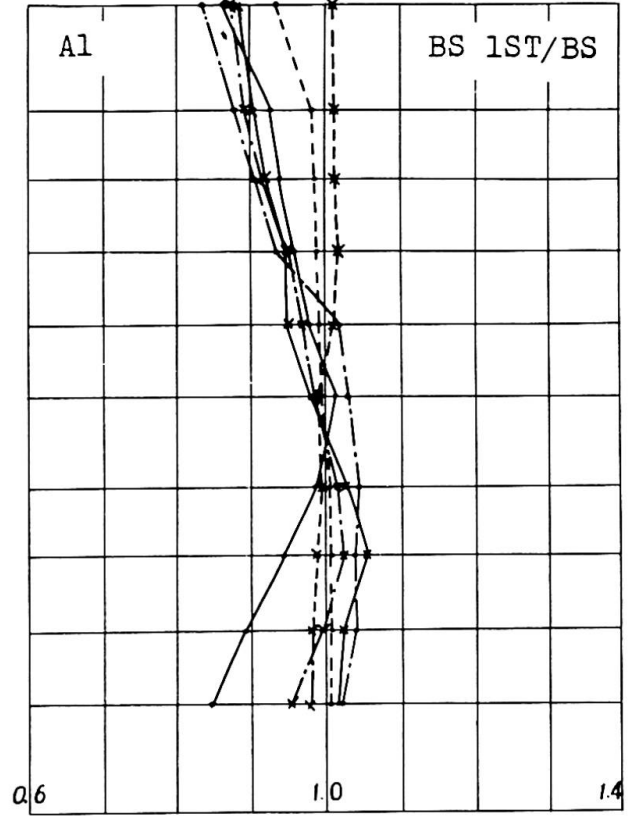
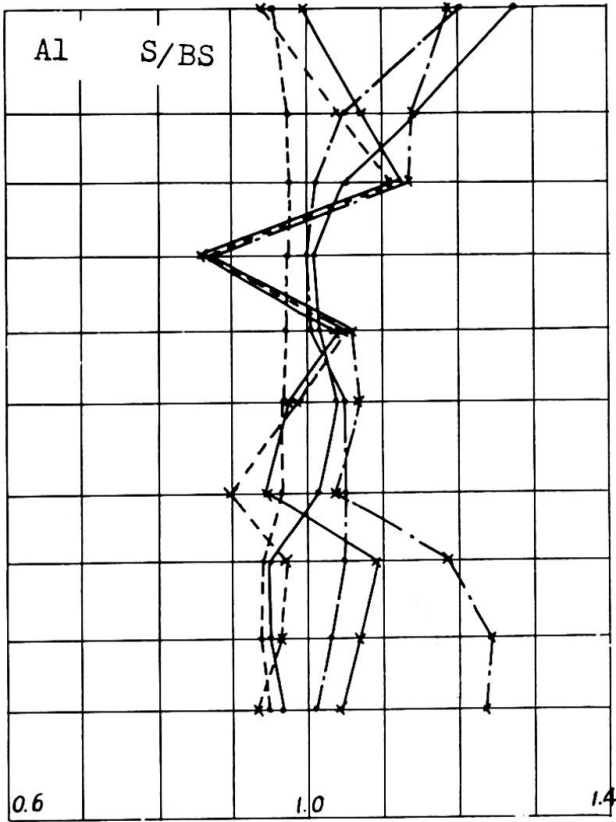
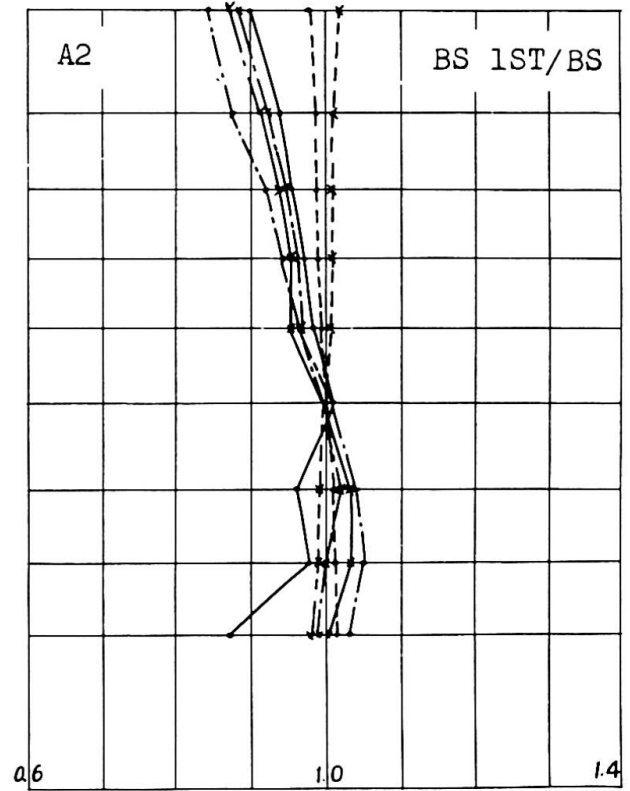
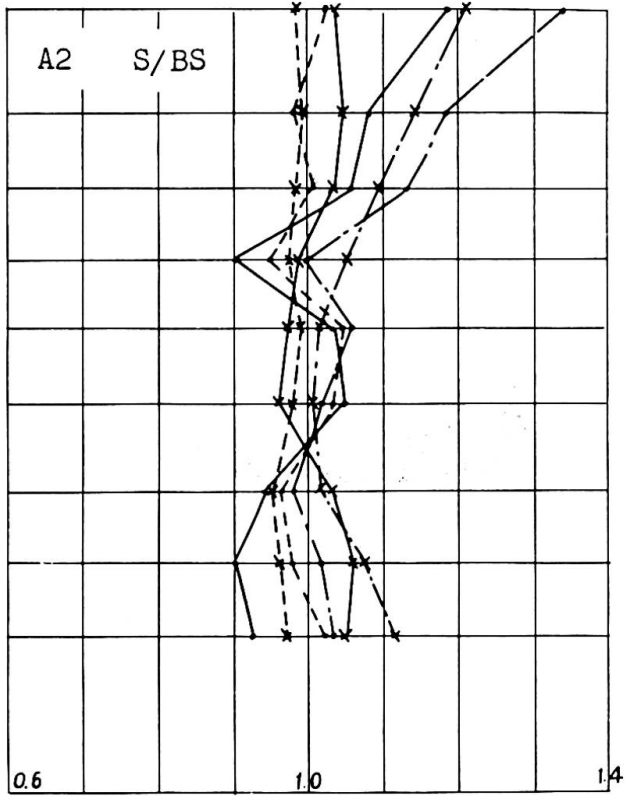


Fig. 11

AKITA
SENDAI
EL CENTRO

$T_1 - 0.663^{sec}$ $T_2 - 0.811$

x-----x
x-----x
x-----x



4. Variation of Response due to Different Modes.

Since the building heretofore discussed (i.e., Example A) is somewhat unusual in Japan in terms of the structural features, two buildings of more common structural design will be discussed as a matter of comparison. These are shown in Fig. 14 and Fig. 15 as Examples B and C respectively, and their responses have been analyzed by assuming an equivalent 5-mass point system of shear type.

In order to enable to investigate the characteristic of response to vibration of different modes on a comparative basis, the natural periods were taken at 0.663 second which was the period for the 1st mode of Frame A₁ and at 0.811 second which was the period for the 1st mode of Frame A₂.

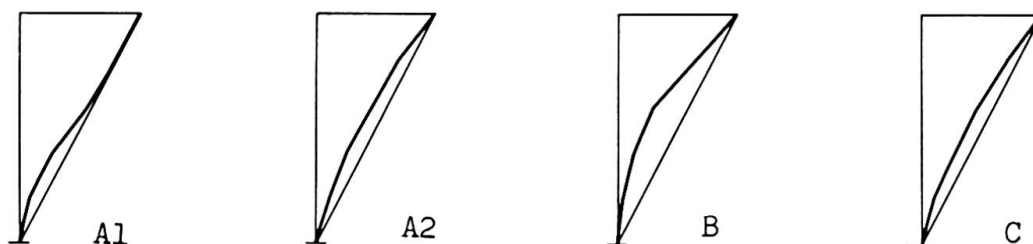


Fig. 12 FIRST MODE OF FOUR CASES

The modes of vibration obtained for the Frames A₁, A₂, B and C are shown in Fig. 12, and the response values in terms of shear force coefficient are shown in Fig. 13.

Considerations.

The comparative analysis has revealed that Frame B has the response characteristic which is quite different from other three cases evidently due to the effects of the higher mode vibration. The reason for this is presumed to be attributable to the fact that the 1st mode of vibration of Frame B is not linear. Japanese structural engineers should bear in mind that a building with this type of response characteristics often results if the building is designed faithfully in accordance with the lateral loads set forth in the Japanese national building code but in disregard of the building's vibration characteristics. The shear force coefficients widely vary with the types of earthquakes adopted for the analysis. This means that the difference in the spectra of the earthquakes shown in Fig. 2 has been directly reflected in the vibration characteristics. The results of these analyses seem to indicate that there are two "problem areas": one is a design problem which concerns the determination of the natural period of a building; and the other, the analysis problem which concerns the types of earthquakes to be used for the earthquake response analysis.

Acknowledgment.

The authors are gratefully indebted to Dr. H. Umemura, professor of structural engineering at Tokyo University for the guidance and help he extended to the authors both during the design of the building discussed here and during the preparation of this present paper.

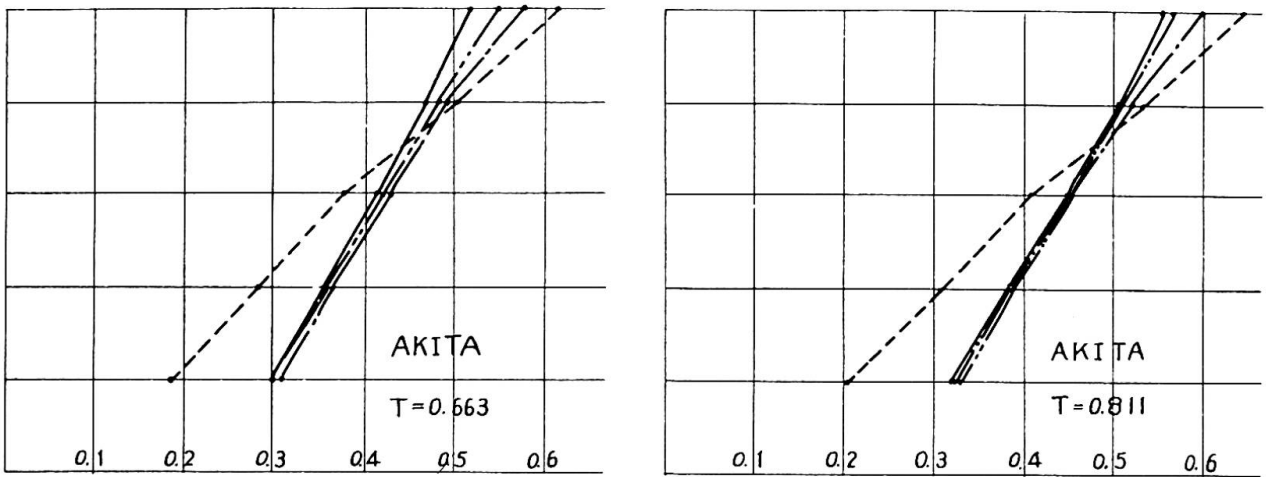
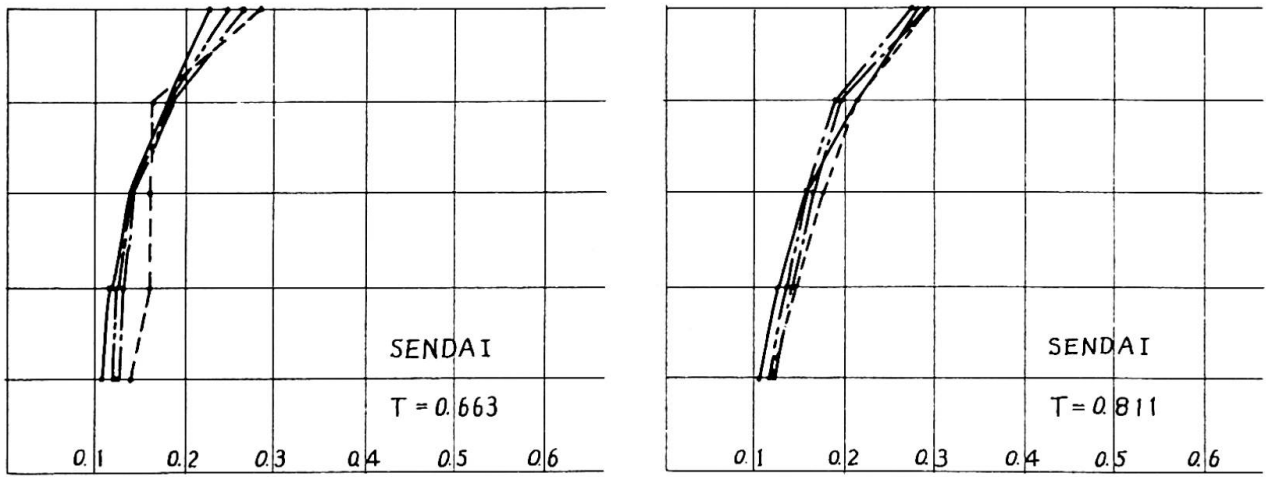
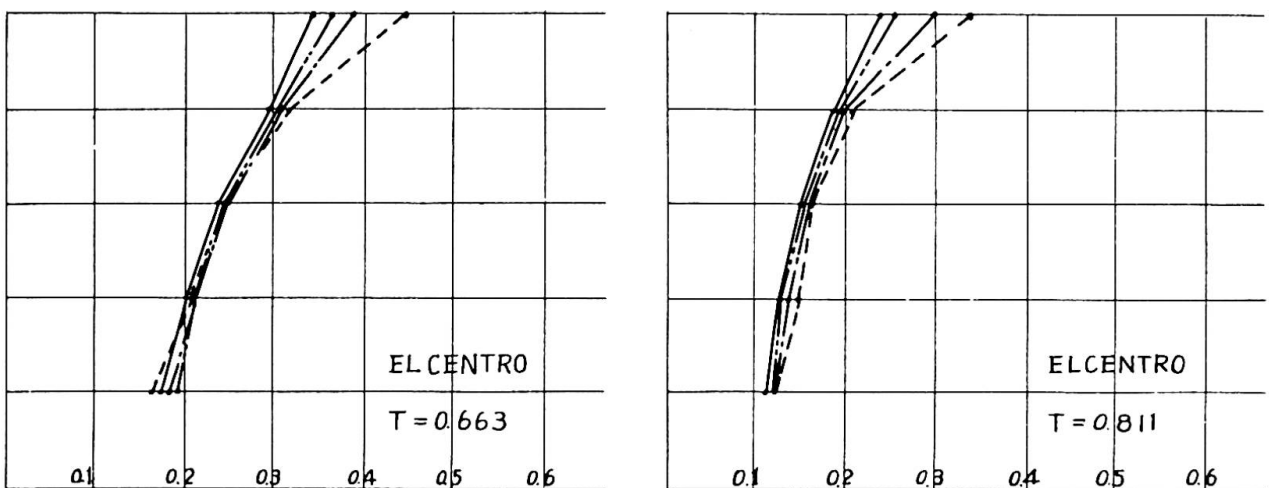
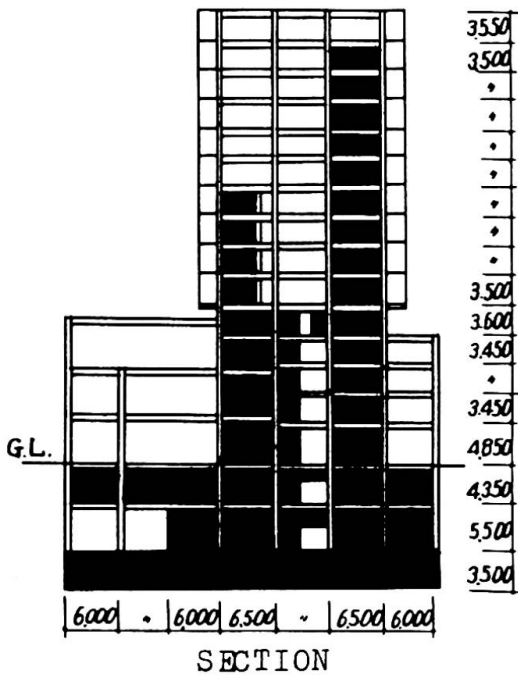


Fig. 13



A1	—————	B	-----
A2	- · - · - · -	C	— · — · —



SECTION
Designed in 1963

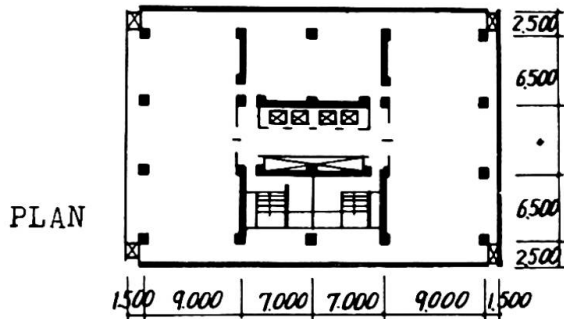
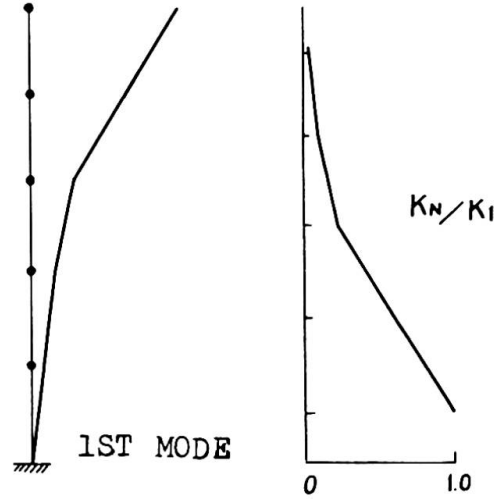
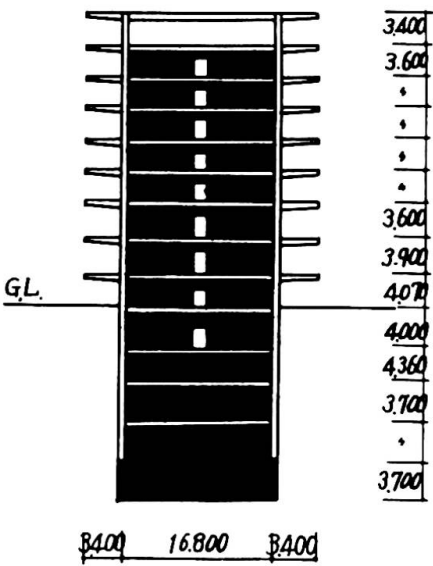


Fig. 14 CASE B



SECTION
Designed in 1964

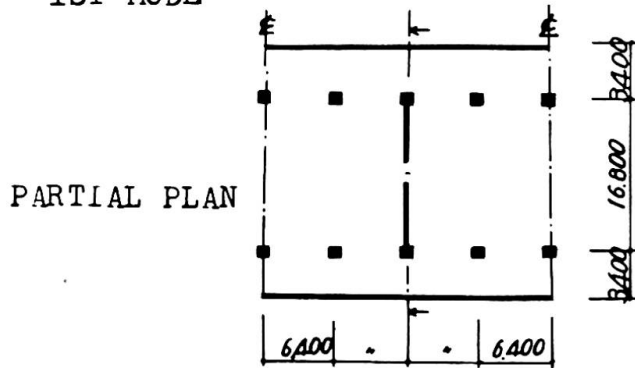
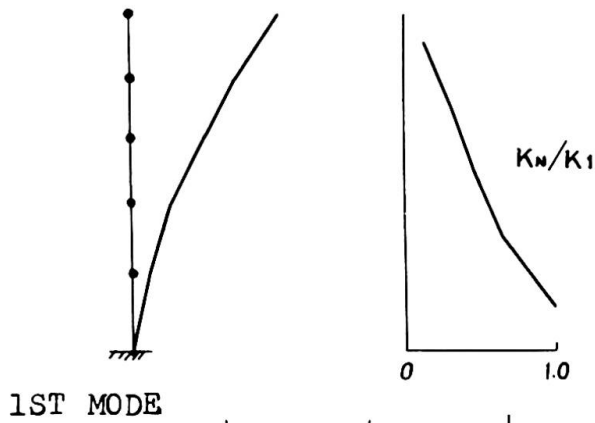


Fig. 15 CASE C

SUMMARY

In an attempt to ascertain the earthquake response characteristics of medium-rise (30 to 45 meters in height) reinforced concrete buildings having shear wall, the authors have made analytical studies on a number of buildings of the type described above. It is hoped that the results of such analyses may serve in future as a source of some useful information for preliminary structural design of similar buildings.

RÉSUMÉ

Pour obtenir des caractéristiques de secousses sismiques dans des constructions de hauteur moyenne (30 - 45 m) en béton armé avec murs de cisaillement, l'auteur a procédé à plusieurs réflexions analytiques. Il espère que les résultats de cette analyse servent à pré-dimensionner des constructions simples.

ZUSAMMENFASSUNG

Der Verfasser hat, in der Absicht Erdbebencharakteristiken an mittelhohen Stahlbetongebäuden von 30 bis 45 Meter mit Schubwänden zu erhalten, einige analytische Ueberlegungen angestellt, hoffend, dass die Ergebnisse dieser Analyse in Zukunft als eine Quelle dienlicher Angaben für den vorläufigen Entwurf einfacher Bauten Verwendung finde.

Vc

Shear Resistance and Explosive Cleavage Failure of Reinforced Concrete Members Subjected to Axial Load

Résistance au cisaillement et rupture cassante explosive d'éléments en béton armé sous charge axiale

Schubwiderstand und explosiver Spröbruch der Stahlbetonsäulen unter Achsiallast

MINORU YAMADA

Professor Dr.-Ing.

Department of Architecture, Faculty of Engineering

Kobe University, Kobe / Japan

SHIGEZO FURUI

Dipl.-Ing.

1. INTRODUCTION

As one of the most essential problem for the ductility requirement of the dynamic behaviour of reinforced concrete buildings, it is discussed here the shear resistance and explosive cleavage failure of reinforced concrete members subjected to axial load. Tests were carried out mainly to make clear the influences of axial load level ratios, shear span ratios and web reinforcement ratios upon their shear resistances and fracture modes. An analytical approach is presented here and compared with test results. By this research, the behaviours of brittle fracture and the causes of the lack of ductility of reinforced concrete members become clear and it will be possible to avoid the explosive cleavage failure, which had caused very often heavy damage of reinforced concrete buildings under strong earthquakes, and to establish the design methods how to give them sufficient ductility.

2. OBJECTIVES and SCOPE

The importance of ductility of members or connections for the dynamic resistance of reinforced concrete structures was emphasized by professors Newmark and Hall⁽¹⁾ in the preliminary publication. The lack of ductility of reinforced concrete members is caused mainly by the presence of high axial load or by the presence of high shearing force.

The former problem was discussed by several researchers⁽²⁾ or by the author⁽³⁾⁽⁴⁾⁽⁵⁾ at the 7th. congress of IABSE. Under higher axial load ($\frac{N}{\sigma_p b D} > 0.5$)⁽⁶⁾, the deformation energy of reinforced concrete beam-column is dissipated mainly by concrete and not by longitudinal reinforcement. Therefore it shows the lack of ductility. On the contrary, under lower axial load ($\frac{N}{\sigma_p b D} < 0.5$), the deformation energy is dissipated mainly by longitudinal reinforcement and so it shows sufficient ductility. The only

way to improve it, is to use sufficient web reinforcement in order to increase the ductility of concrete. There exists not so sufficient ductility by the presence of axial load but the fracture mode is always mild and not so brittle as shear fracture.

On the latter problem there are not yet sufficient knowledge^{[7][8]}. Moreover this problem is more essential for ductility requirements, because the fracture mode under higher shearing force shows a very brittle nature, and that it shows often even explosive fracture, especially in the presence of axial compression (see Photo. 1). There exists no ductility and yet such a fracture mode were found very often in heavily damaged reinforced concrete buildings under strong earthquake motion. They had caused often the collapse of whole structures at earthquake (see Photo. 2).

This paper deals on the fracture mode of reinforced concrete members subjected to high shearing force under axial compression and on the contribution of web reinforcements for this explosive cleavage failure. Tests were carried out to make clear the influences of axial load level ratios, shear span ratios and web reinforcement ratios of reinforced concrete members upon the shear resistance and shear fracture modes of them. An analytical treatment, which is based upon the biaxial fracture criteria of concrete, is presented here and compared with test results.

3. TESTS

3-1. Test Procedures and Measuring Devices

Tests were carried out by loading frames, which were specially installed in testing machine as shown in Fig. 1. The constant axial compression load $N (=X \cdot N_0)$ was introduced by testing machine through roller and maintained steady at constant value throughout the test. The transverse load P was applied by oil jack with electric load cell at its head, which was installed in loading frames.

There were two loading systems for shear tests as shown in Fig. 2, i.e. type C with single curvature in uniform shear span "a" at the both ends of the specimen and type Z with double curvature in uniform shear span "2a" at the central part of the specimen. Type C is ordinary shear mechanism for beam test and it has a merit of ordinary case as beam but has a demerit of the influences of additional bending through axial load by deflection for column test. Type Z is a special mechanism for shear test and it has a merit for the case of column test to avoid the influences of additional bending through deflection and to make possible the tests under higher shear span ratios. This loading system simulate often the loading condition of columns, beams or beam to column connections under earthquake motion.

Longitudinal and transverse displacements between main points or diagonal displacements between diagonal points in test span were measured by 1/100 mm dial gauges, which were set in measuring frame, that was fixed at one end on one loading line. Wire strain gauges were pasted upon surfaces in test span or several other deformation measuring techniques like checkerboard printing on the testing surfaces were applied them too.

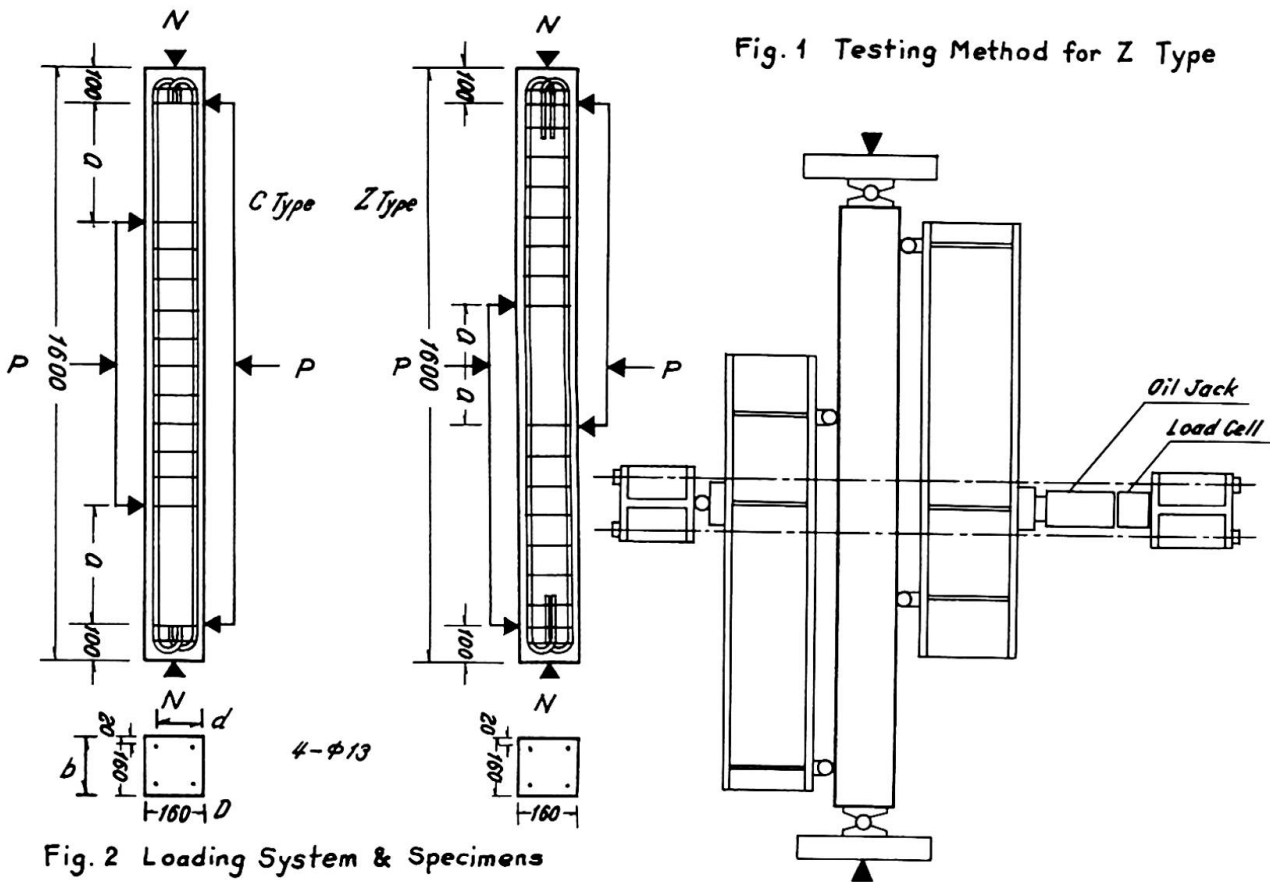


Fig. 1 Testing Method for Z Type

Fig. 2 Loading System & Specimens

3-2. Test Specimens and Test Series

Specimens had a length of 160 cm with a square cross section of width and depth of 16 cm x 16 cm and reinforced with 4 ordinary round steel bars of 13 mm diameter for longitudinal reinforcement, i.e. longitudinal gross reinforcement ratio $\rho_g = 1.04\%$. Test spans were reinforced with or without web reinforcement according to test series. Other spans were reinforced with web reinforcement of square type hoop of ordinary round steel bars of 6 mm diameter with 8 cm pitches (see Fig. 2). Both ends of web reinforcement were welded together.

Concrete mix is 1 : 2.55 : 3.34 and $W/C = 60\%$, the approximate concrete compressive strength $\sigma_c \cong 200 \text{ kg/cm}^2$, the approximate concrete tensile strength $\sigma_t \cong 20 \text{ kg/cm}^2$, the approximate yield point of longitudinal reinforcement of $\phi 13$, $\sigma_y \cong 2800 \text{ kg/cm}^2$ or 3045 kg/cm^2 and of web reinforcement of $\phi 6$, $\sigma_{yw} \cong 2144 \text{ kg/cm}^2$. The mechanical properties of materials are shown in Table 1.

Tests were carried out in three series:

- Series I : For the research of the influence of shear span ratios upon shear behaviour, comparison between test mechanisms C type and Z type. The shear span ratio of Z type is defined here a/d . In this project the shear span ratios were varied 0.6 1.2 1.8 2.4 for Z type and 1.2 2.4 3.6 4.8 for C type. Test spans were not reinforced with web reinforcement.
- Series II : For the research of the influences of the axial load level ratios upon shear behaviour. The axial

load level ratio $X(= \frac{N}{N_0})$ is defined here as the ratio of acting constant axial compression N versus ultimate strength of centrally loaded column N_0 . There were varied 0 (beam), 1/6 and 1/3. Test spans were not reinforced with web reinforcement.

Series III : For the research of the contribution of web reinforcement. As web reinforcement it was applied here a square type hoop of round steel bar with 6 mm diameter. The hoop spacings were varied 0, 16 cm, 8 cm, 4 cm, i.e. web reinforcement ratios $\eta = 0, 0,22, 0,44, 0,88\%$. It is defined here as the ratio of the area of longitudinal cross section of concrete versus the area of web reinforcement. contained in that cross section (see Fig. 4).

Series I and II were tested together. They are shown in Table 1.

3-3. Test Results

Test results are summarized in Table 1. Numerals following to B in the specimen notation of the table indicate the hoop spacing in cm and C or Z with numerals

indicate the test mechanism and the ratio of the shear span versus the depth of specimen. The fracture mode S in the table indicates cleavage shear explosion, B → S indicates initially bending and finally shear crack opening and B indicates bending crack deformation.

The deformation process and fracture modes under various shear span ratios and various axial load level ratios are shown in Fig. 3, as the relation between relative displacements of both ends of shear span "2a" for Z type and lateral load P.

Z.R. in the figures of deformation characteristics indicates the formation of tensile crack, S.R. the formation of shear crack opening, L.R. the formation of a diagonal tension crack between loading points and X-mark the explosive cleavage shear

Table 1 Test Series & Test Results

Specimen	o/d	Steel		Concrete		Const. Axial Load	Max. Bending Moment	Max. Shear Force	Fracture Mode
		σ_y kg/cm^2	Comp. σ_c	Tens. σ_z	Comp. σ_c				
RC:C1:B0:C1:1/3NoQ	1.2	2800	291	24.7	30t	1.95tm	12.2t	S	
RC:C1:B0:C2:1/3NoQ	2.4	2800	360	27.7	36	2.24	7.00	B	
RC:C1:B0:C3:1/3NoQ	3.6	2800	360	27.7	36	2.30	4.79	B	
RC:C1:B0:C4:1/3NoQ	4.8	2800	360	27.7	36	2.40	3.75	B	
RC:C1:B0:C3:1/6NoQ	3.6	2800	360	27.7	18	1.96	4.10	B	
RC:C1:B0:C3:0NoQ	3.6	2800	360	27.7	0	1.00	2.09	B	
RC:C1:B0:Z1:1/3NoQ	0.6	2800	291	24.7	30	1.05	12.7	S	
RC:C1:B0:Z2:1/3NoQ	1.2	2800	291	24.7	30	1.60	9.40	S	
RC:C1:B0:Z3:1/3NoQ	1.8	2800	291	24.7	30	2.29	9.50	S	
RC:C1:B0:Z4:1/3NoQ	2.4	2820	218	19.7	24	1.97	6.17	B→S	
RC:C1:B0:Z1:1/6NoQ	0.6	3045	213	19.7	12	0.73	9.10	S	
RC:C1:B0:Z2:1/6NoQ	1.2	3045	213	19.7	12	1.12	7.00	S	
RC:C1:B0:Z3:1/6NoQ	1.8	3045	213	19.7	12	1.70	7.10	S	
RC:C1:B0:Z4:1/6NoQ	2.4	3045	213	19.7	12	1.92	6.00	B→S	
RC:C1:B0:Z1:0NoQ	0.6	3045	197	19.4	0	0.53	6.60	B→S	
RC:C1:B0:Z2:0NoQ	1.2	3045	197	19.4	0	1.04	6.50	B→S	
RC:C1:B0:Z3:0NoQ	1.8	3045	197	19.4	0	0.91	3.80	B→S	
RC:C1:B0:Z4:0NoQ	2.4	3045	197	19.4	0	1.25	3.90	B	
RC:C1:B0:Z3:0NoQ	1.8	2800	291	24.7	0	1.15	4.80	B→S	
RC:C1:B4:Z2:1/3NoQ	1.2	2800	202	20.2	23	1.81	11.3	B→S	
RC:C1:B8:Z2:1/3NoQ	1.2	2800	202	20.2	23	1.51	9.42	S	
RC:C1:B16:Z2:1/3NoQ	1.2	2800	202	20.2	23	1.38	8.66	S	
RC:C1:B0:Z2:1/3NoQ	1.2	2800	202	20.2	23	1.13	7.06	S	

B: Bending Fracture
 S: Cleavag Shear Fracture (Explosion)
 B→S: Bending → Shear Crack Opening

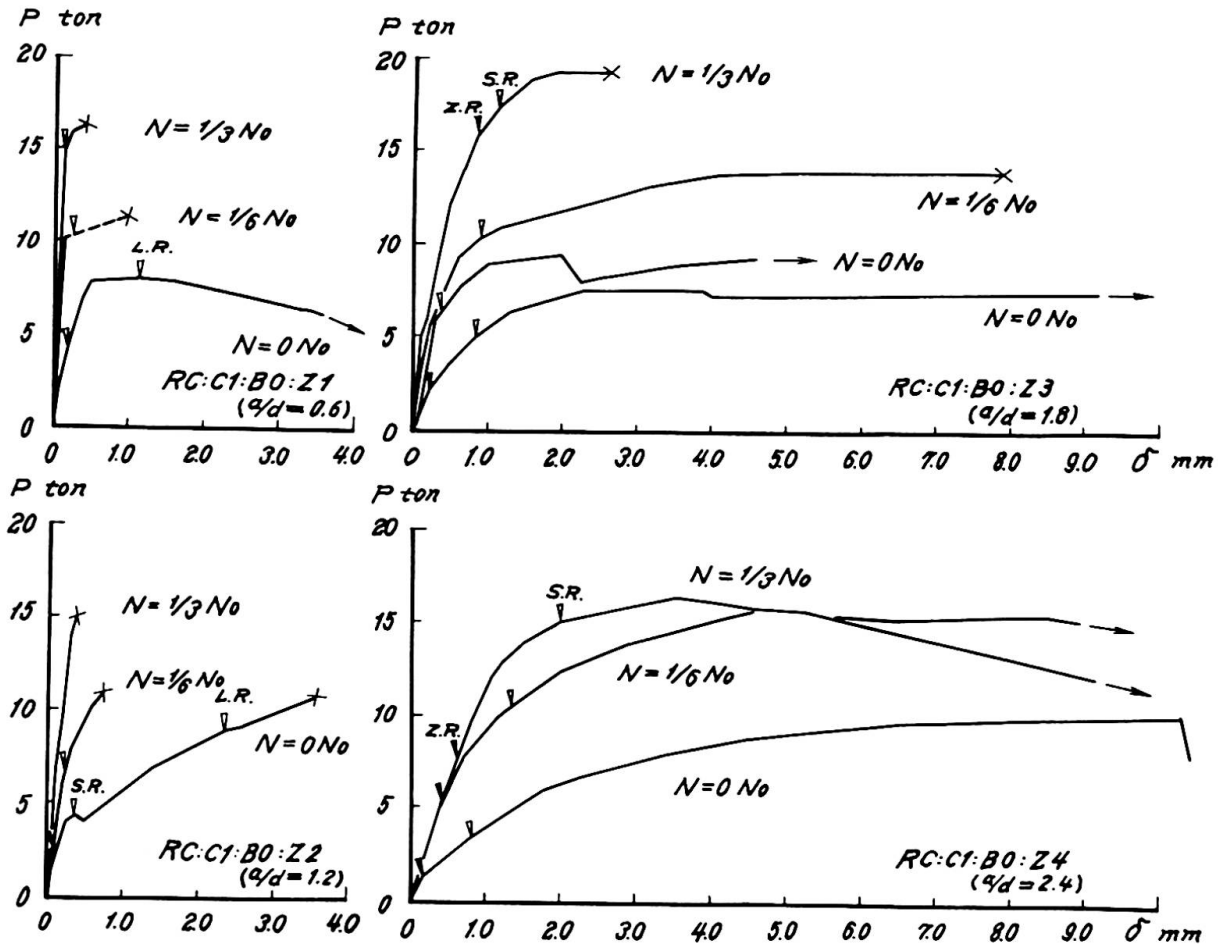


Fig.3 Deformation Characteristics

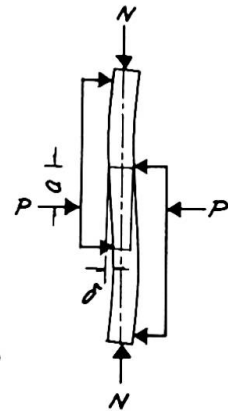
failure.

Under higher shear span ratios it appears at first bending crack Z.R. at the tension side of the loaded cross section and the deformation occurs mainly by the opening of this tensile crack, then this tensile crack shows inclination or it appears several shear cracks S.R. and finally the compression side of the loaded cross section is crushed down.

Under intermediate shear span ratios it appears initially tensile crack Z.R. by bending at the tension side of the loaded cross section, then on the side surfaces of shear span it appears short diagonal cracks and its opening becomes larger.

Under lower shear span ratios it appears initially several short shear cracks on the side surfaces of shear span and gradually it increases their number accompanied by the increase of transverse load, then suddenly but in several seconds it occurs explosion by a large diagonal tension crack opening directly between loading points independently from formerly formed short shear cracks. This behaviour is intensiver, the higher the axial load ratios (see Photo.1).

The deformation process and fracture modes, for the case of a shear span ratio of 1,2 and an axial load level ratio of 1/3 with various web reinforcement ratios are shown in Figs. 4 and 12.



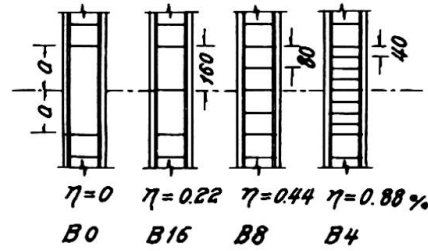
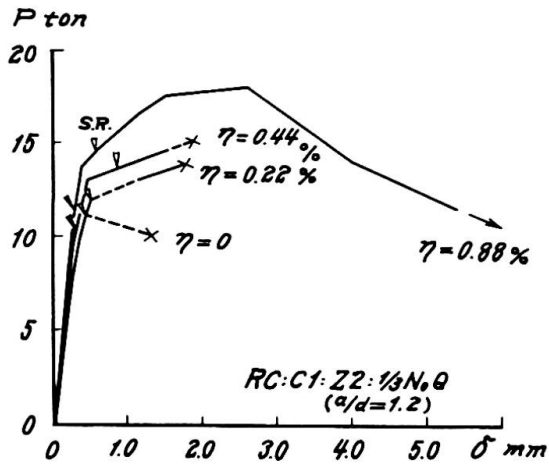


Fig.4 Contribution of Web Reinforcement for Shear Deformation & Fracture

4. ANALYTICAL APPROACH

4-1. General Description

For the analysis, the reinforced concrete member is divided into finite small rectangular elements with a central point (i, j) as their co-ordinates. The stresses and displacements of each element are represented by this cross point. Following to the increase of external load, the stresses and displacements are calculated and the fracture of each element is checked by critical fracture condition of concrete. If the stress condition of one element reaches the critical condition, the element is destroyed and it bears no more stresses and the stresses, which were born by the failed element, will be redistributed to another elements proportional to their stiffness. After the redistribution of stresses, it proceeds to next loading stage. So by repeating this procedure step by step, the elasto-plastic deformation behaviour of this member is able to followed. Through the decrease of the number of load bearing elements, finally it will bear no more increase of external load and it will reach the ultimate state. Fracture mode and ultimate strength will be so clarified.

4-2. Elements and their Fracture Condition

For the stresses and displacements of an element, it is assumed that:

- (1) As the element, there are two kinds of elements, i.e. concrete element with reinforcing steel and concrete element without reinforcing steel. Reinforcing steel is estimated by equivalent cross section for normal stresses.
- (2) The external forces are distributed to each elements proportional to their stiffness. They are represented with their central point. As the stresses of each element, it is considered σ_{ij} and τ_{ij} but it is neglected here the normal stresses perpendicular to the member axis.
- (3) The shearing stress τ_{ij} is decided by normal stress and for the element with reinforcing steel it is considered the

increment of shearing stress by the difference of stresses in reinforcing steel.

The displacements of each cross point are: (see Fig. 5)

$$V_{ij+1} = -\beta \cdot a \left[\frac{\sigma_{ij} + \sigma_{ij+1}}{2} \cdot \frac{1}{E_c} \right] + V_{ij} \quad (1), \quad \varphi_{ij} = \frac{V_{i+1,j} - V_{ij}}{\alpha \cdot D} \quad (4),$$

$$V_{i+1,j+1} = -\beta \cdot a \left[\frac{\sigma_{i+1,j} + \sigma_{i+1,j+1}}{2} \cdot \frac{1}{E_c} \right] + V_{i+1,j} \quad (2), \quad \theta_{ij} = -(\delta_{ij} + \varphi_{ij}) = \theta_{i+1,j} \quad (5),$$

$$\sigma_{ij} = \frac{\tau_{ij} + \tau_{i+1,j} + \tau_{i,j+1} + \tau_{i+1,j+1}}{4} \cdot \frac{1}{G_c} \quad (3), \quad u_{ij+1} = \beta \cdot \alpha \cdot \theta_{ij} + u_{ij} \quad (6).$$

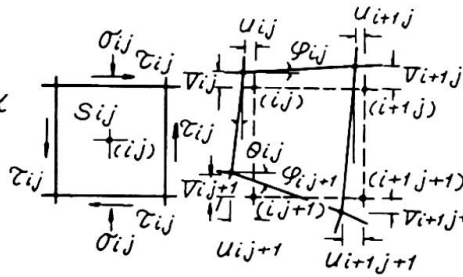
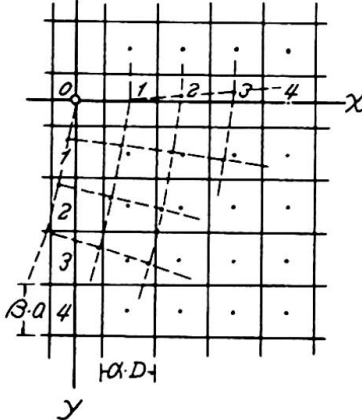


Fig. 5 Finite Element

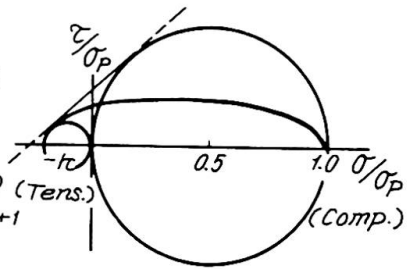


Fig. 6 Fracture Condition of Concrete

The critical fracture condition of each element is assumed to occur under the following combined biaxial fracture condition of concrete by Mohr (see Fig. 6):

$$\frac{(1+K)^2}{K} \cdot \tau^2 + \left[\sigma - \frac{(1-K)}{2} \sigma_p \right]^2 = \frac{(1+K)^2}{4} \cdot \sigma_p^2 \quad (7),$$

here, $K = \sigma_z / \sigma_p$, σ_z and σ_p tensile and compressive strength of concrete respectively.

The normal stress σ and the shearing stress τ for the estimation of the critical condition of the element, which are influenced by redistribution of stresses from neighbouring elements, are calculated as follows:

$$\sigma = \frac{\sigma_{i-1} + 2\sigma_{ij} + \sigma_{i+1}}{4} \quad (8),$$

$$\tau = \frac{\tau_{i-1,j} + 2\tau_{ij} + \tau_{i+1,j}}{4} \quad (9).$$

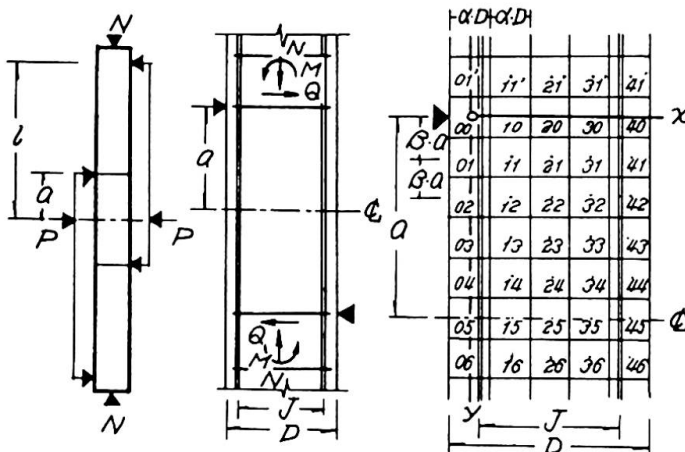


Fig. 7 Reinforced Concrete Member

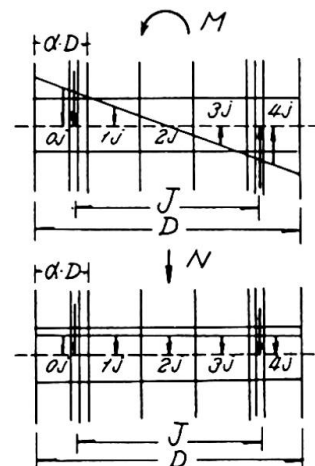


Fig. 8. Normal Stresses

4-3. Application for Reinforced Concrete Columns loaded by Bending Moment, Shearing Force and Axial Compression

Normal stress of each element is calculated as the sum of normal stresses $N\sigma_{ij}$ through bending moment and $N\sigma_{ij}$ through axial

load. Within each element the stress is assumed to distribute uniformly. The steel stress is calculated by the concrete normal stress σ_{ij} , in which element the reinforcing steel is contained (S_{ij} , S_{nj} in Fig. 8), and if the reinforcing steel is placed excentrically to the center of the cross point, it is modified by the equivalent ratio of moduli of elasticity n' as follows:

$$\sigma_{sij} = n' \cdot \sigma_{ij} , \quad (n = E_s/E_c , \quad n' = \frac{d/2}{2\alpha \cdot D} \cdot n) \tag{10}$$

So the normal stress through bending moment is calculated by the equilibrium condition as follows:

$$n\sigma_{ij} \cdot (\alpha \cdot D \cdot b + n' \cdot A_s) + n\sigma_{ij} \cdot \alpha \cdot D \cdot b + n\sigma_{2j} \cdot \alpha \cdot D \cdot b + n\sigma_{3j} \cdot \alpha \cdot D \cdot b + n\sigma_{4j} (\alpha \cdot D \cdot b + n' \cdot A_s) = 0 \tag{11}$$

$$n\sigma_{ij} (2\alpha^2 D^2 b + n' A_s \cdot d/2) + n\sigma_{ij} \cdot \alpha^2 D^2 b - n\sigma_{3j} \cdot \alpha^2 D^2 b - n\sigma_{4j} (2\alpha^2 D^2 b + n' A_s \cdot d/2) = M_j \tag{12}$$

Normal stress $n\sigma_{ij}$ by axial compression is calculated by the ratio of moduli of elasticity n as follows:

$$n\sigma_{ij} \cdot \alpha \cdot D \cdot b = \frac{\alpha \cdot D \cdot b \cdot E_c}{(5 \cdot \alpha \cdot D \cdot b + 2n \cdot A_s) E_c} \cdot N \tag{13}$$

Shearing stress τ_{ij} is calculated for the element without longitudinal reinforcement:

$$\tau_{ij} = \frac{1}{2} \left[\frac{(n\sigma_{ij-1} + n\sigma_{ij-1}) - (n\sigma_{i,j+1} + n\sigma_{i,j+1})}{2} + \frac{(n\sigma_{i-1,j-1} + n\sigma_{i-1,j-1}) - (n\sigma_{i-1,j+1} + n\sigma_{i-1,j+1})}{2} \right] \cdot \frac{\alpha \cdot b \cdot D}{\beta \cdot a \cdot b} + \tau_{i-1,j} \tag{14}$$

and for the element with longitudinal reinforcement:

$$\tau_{ij} = \frac{1}{2} \left[\frac{n\sigma_{ij-1} - n\sigma_{i,j+1}}{2} + \frac{n\sigma_{i-1,j-1} - n\sigma_{i-1,j+1}}{2} \right] \cdot \frac{\alpha \cdot b \cdot D + n' \cdot A_s}{\beta \cdot a \cdot b} + \frac{1}{2} \left[\frac{n\sigma_{ij-1} - n\sigma_{i,j+1}}{2} + \frac{n\sigma_{i-1,j-1} - n\sigma_{i-1,j+1}}{2} \right] \cdot \frac{\alpha \cdot b \cdot D + n' \cdot A_s}{\beta \cdot a \cdot b} + \tau_{i-1,j} \tag{15}$$

Through the fracture of each element, the stresses are re-distributed. If the element S_{nj} in Fig. 9 is destroyed, the element S_{nj} bears now only by longitudinal steel and therefore the stiffness of S_{nj} for normal stress decreases. Then the neutral axis removes towards the compression side and through the equilibrium condition the new normal stress σ_{ij} is decided. Shearing stresses in $S_{i,j-1}$ and $S_{i,j+1}$ are redistributed by (14) and (15).

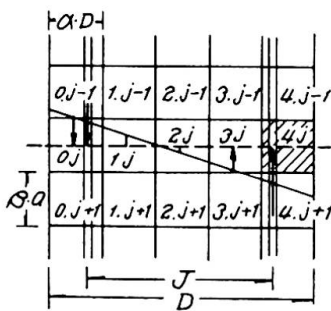


Fig. 9 Destroyed Element

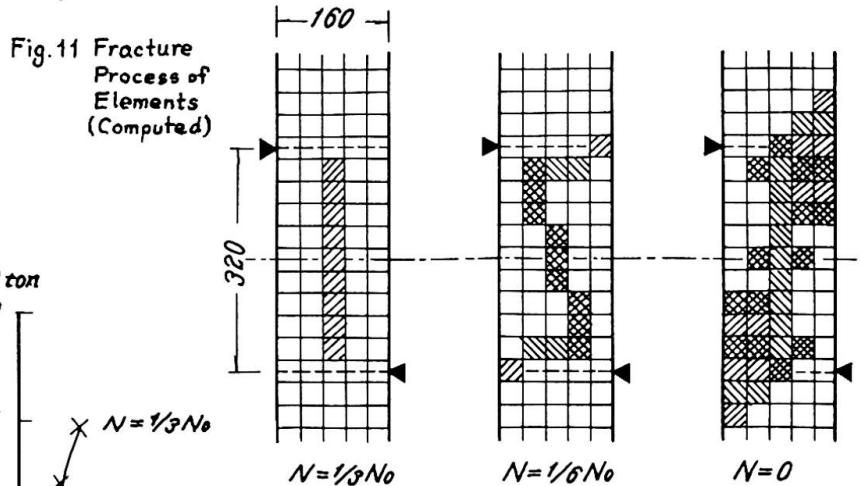


Fig. 10 Fracture Process of RC:C1:B0:Z2 (Measured & Computed).

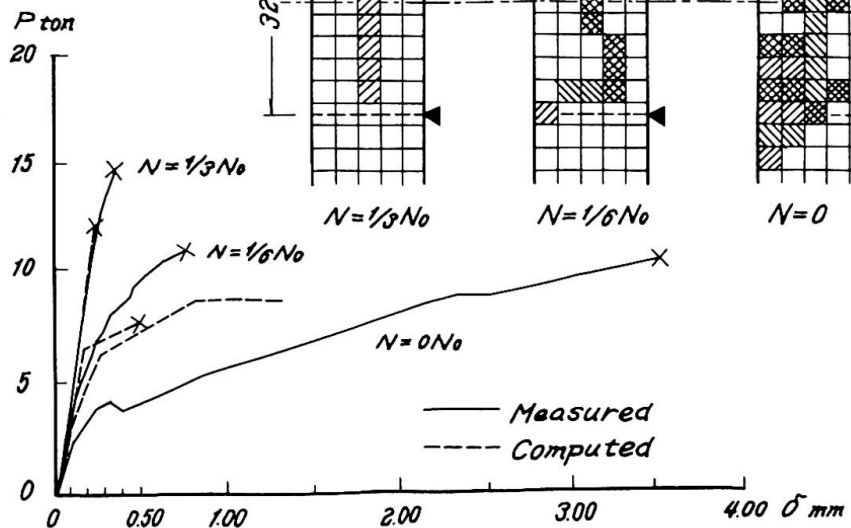


Fig. 10 shows the test results with solid lines and corresponding calculated values of foregoing deformation analysis for the case of a shear span ratio $a/d=1,2$ and axial load level ratios of 0, $1/6$ and $1/3$ with dotted lines.

Fig. 11 shows the fracture process of foregoing analysis. For the case of $N=\frac{1}{3}N_0$, the elements in the central part of the member is destroyed through compressive shear and the redistributed stresses destroyed another elements one after another and it increases no more load bearing capacity. For the case of $N=\frac{1}{6}N_0$, at first the extreme tension side element reaches the critical condition at the maximum moment section and then, following to the increase of external load, the inside elements are destroyed gradually and final state is decided. For the case of $N=0N_0$, at first the tensile crack occurs and it penetrates into inside and, even when the central elements are destroyed by tensile shear, it shows the more increase of load carrying capacity.

5. DISCUSSIONS

5-1. Interaction between Shear Span Ratios and Axial Load Ratios

Table 2 shows the interaction between shear span ratios (a/d) and axial load level ratios ($X=\frac{N}{N_0}$) upon the fracture behaviours of reinforced concrete members very clearly. The lower the shear span ratios and the higher the axial load ratios becomes the explosiver the fracture mode. On the contrary, the higher the shear span ratios and the lower the axial load ratios, the milder the fracture mode. The ductility of members is influenced and decided by this fracture mode. Ductility requirement of reinforced concrete members is satisfied under the condition of lower axial load ratios and higher shear span ratios.

It is a remarkable fact that there exists a very clear difference of fracture modes at a value of (a/d) between 1,8 and 2,4 for every axial load ratios. (See Photo. 3)

Bending resistance decreases under lower shear span ratios for columns as it was pointed out for beams by prof. Kani[9].

Table 2. Interaction $a/d - X$

a/d	Constant Axial Load Ratio		
	$N=0N_0$	$N=\frac{1}{6}N_0$	$N=\frac{1}{3}N_0$
0.6	$B \rightarrow S$	S	S
1.2	$B \rightarrow S$	S	S
1.8	$B \rightarrow S$	S	S
2.4	B	$B \rightarrow S$	$B \rightarrow S$

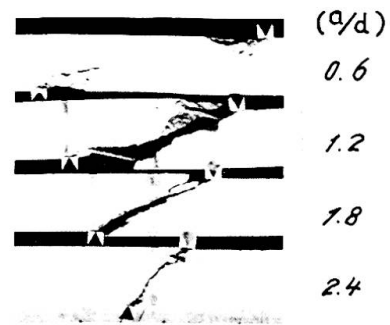


Photo. 3 Influences of Shear Span Ratios (a/d) upon the Fracture Modes ($\eta=0, N=\frac{1}{3}N_0$)

5-2. Effect of Web Reinforcement

Ductility requirement under higher axial load ratios with lower shear span ratios is improved by web reinforcement. The effects are shown in Fig. 4 under an axial load level ratio of $1/3$ and a shear span ratio of 1,2. It is a very severe condition, but it happens often in actual case, for the case of without web reinforcement $\eta=0$, it shows a typical explosive shear fracture. For the case with lower web reinforcement ratios $\eta=0,22$ and $0,44\%$, they showed a little ductility even with a little increase of resistance, but finally explosive cleavage failure. However for the case with fairly higher web reinforcement ratio $\eta=0,88\%$, it shows no more shear fracture but

sufficient ductility.

5-3. Damage of Reinforced Concrete Buildings under Strong Earthquakes

Photo. 2 shows one of the typical cleavage shear fracture of a reinforced concrete column of the gymnasium of Niigata high school, at the strong earthquake on the 16th. June 1964, Niigata/Japan. Photos 1 and 2, i.e. test specimen and real case show a very good similarity of their fracture mode. Test specimen shows the cause of damage of reinforced concrete columns under earthquake very clearly. Such a explosive cleavage shear failure of column caused very often heavy damage of whole buildings under strong earthquakes. These photographs of damage under earthquake show very clearly the importance of the problem of shear resistance under axial compression for the dynamic behaviour of reinforced concrete buildings.

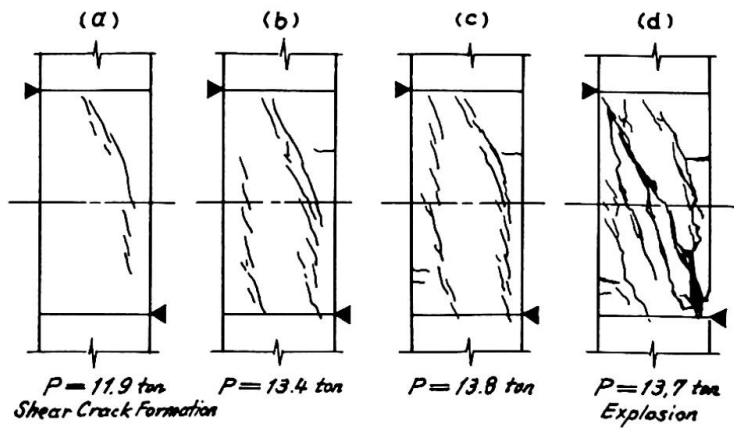
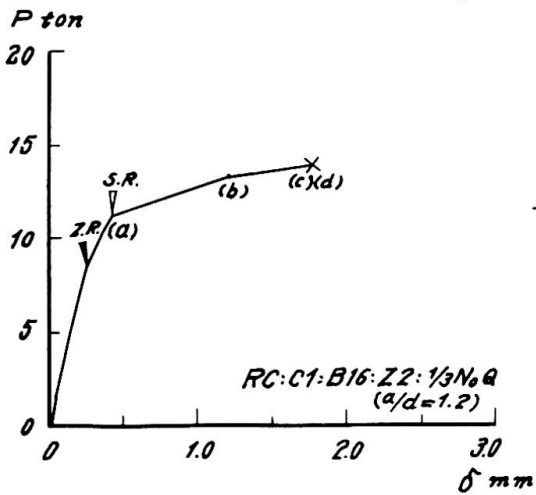


Fig. 12 Formation of Shear Cracks and Explosive Cleavage Failure (a/d=1.2, η=0.22, N=1/3No.)

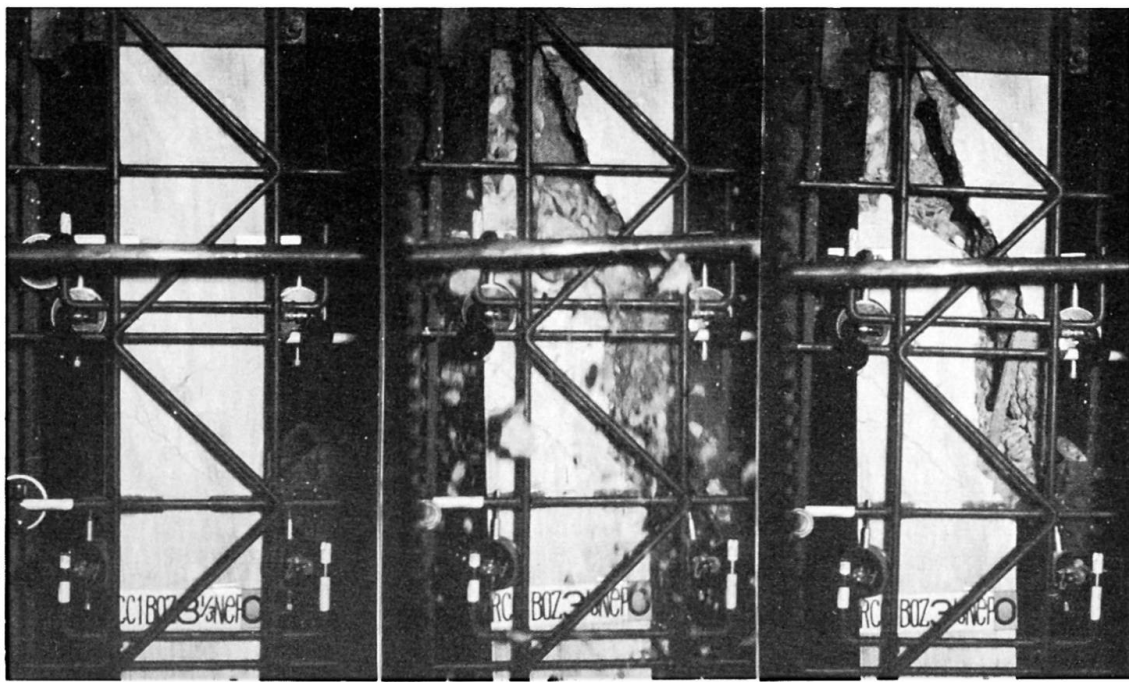


Photo. 1 Cleavage Explosive Shear Fracture of Reinforced Concrete Columns. (a/d = 1.8, η = 0, N = 1/3No.)

Photo. 2 Cleavage Shear Fracture of a Reinforced Concrete Column of Gymnasium in Niigata High School / Japan, by the Earthquake on the 16th. June, 1964.
(Photo.: Courtesy of ass.Prof. Mizuhata)



6. CONCLUDING REMARKS

The lack of ductility of reinforced concrete member is caused by high axial compression and high shear force. The simultaneous action of both forces had caused very often heavy damage of whole structures under strong earthquakes (see Photo. 2).

This paper intends to make clear the shear resistance and explosive cleavage failure of reinforced concrete members subjected to axial load as one of the most essential cause of the lack of ductility. Three series of tests were carried out to make clear the influences of axial load level ratios, shear span ratios and web reinforcement ratios upon deformation characteristics and fracture modes. Test results are shown in Figs. 3 and 4 and summarized in Tables 1 and 2. They show the fact that the higher the axial load level ratios, the lower the shear span ratios and the lower the web reinforcement ratios, the ductility of the member will be lost and it causes often explosive cleavage failure (see Photo. 1). Test specimens show a very good simulation with actual case under earthquake.

An analytical approach gives a fairly good agreement with the behaviours of test results (Figs. 10, 11).

7. REFERENCES

- [1] Newmark, N.M., Hall, W.J.: Dynamic Behaviour of Reinforced and Prestressed Concrete Buildings under Horizontal Forces and the Design of Joints, Prel. Publ., 8th. Congress, IABSE, pp.585/613.
- [2] Flexural Mechanics of Reinforced Concrete, Proc., Internl. Symposium, Miami, Fla./Nov. 1964, ASCE-ACI.
- [3] Yamada, M.: Drehfähigkeit Plastischer Gelenke in Stahlbeton balken, Beton- u. Stahlbetonbau, H.4. Apr. 1958, pp.85/91.

- [4] Yamada, M.: Verhalten Plastischer Gelenke in Stahlbetonbalken, Prel. Publ., 7th. Congress, IABSE, 1964, pp.963/970.
- [5] Yamada, M.: Verhalten Plastischer Gelenke in Stahlbetonsäulen, Finl. Publ., 7th. Congress, IABSE, 1964, pp.481/488.
- [6] Yamada, M., Kawamura, H.: Elasto-Plastische Biegeformänderungen der Stahlbetonsäulen und-balken, Abh., IVBH, Bd. 28/I.
- [7] Morrow, J., Viest, I.M.: Shear Strength of Reinforced Concrete Frame Members Without Web Reinforcement, J., ACI., Mar. 1957, pp.833/869.
- [8] Baldwin, J.M.Jr., Viest, I.M.: Effect of Axial Compression on Shear Strength of Reinforced Concrete Frame Members, J., ACI, Nov. 1958, pp.635/654.
- [9] Kani, G.N.J.: The Riddle of Shear Failure and Its Solution, J., ACI., Apr. 1964, pp.441/467.
- [10] Leonhardt, F., Walter, R.: Beiträge zur Behandlung der Schubprobleme in Stahlbetonbau, Beton- u. Stahlbetonbau.
- [11] Thülimann, B.: General Report, IVa, Shear Strength, Reinforced and Prestressed Concrete, Prel. Publ., pp.747/750, Finl. Publ., pp.311/315, 7th. Congress, IABSE, 1964.
- [12] Rüsck, H.: Über eine Erweiterung der Mörschen Fachwerk-analogie, Finl. Publ., 7th. Congress, IABSE, 1964, pp.353/369.
- [13] Wästlund, G.: A Theory of Combined Action of Bending Moment and Shear in Reinforced and Prestressed Concrete Beams, Finl. Publ., 7th. Congress, IABSE, 1964, pp.371/377.

SUMMARY

As one of the most essential problem for the ductility requirement of the dynamic behaviour of reinforced concrete buildings, theoretical and experimental researches were carried out to make clear the influences of axial load ratios, shear span ratios and the contribution of web reinforcement ratios upon the shear resistance and fracture modes. It becomes clear one of the most important cause of the heavy damage of reinforced concrete buildings by the lack of ductility (Photos. 1 and 2).

RÉSUMÉ

Des recherches théoriques et expérimentales ont été faites concernant la ténacité et son influence dans le comportement dynamique de bâtiments en béton armé, pour déterminer l'influence de la charge axiale, de la répartition des forces de cisaillement, et la contribution du réseau d'armature sur la résistance de cisaillement et sur le comportement à la rupture. On voit que le manque de ténacité est une des causes les plus importantes des lourds dommages dans les bâtiments en béton armé. (Fig. 1 et 2)

ZUSAMMENFASSUNG

Als eines der wichtigsten Probleme für die Zähigkeitsforderung des dynamischen Verhaltens von Stahlbetongebäuden wurden theoretische und experimentelle Untersuchungen angestellt, um den Einfluss der Achsialkraft, der Querkraftverteilung sowie des Bewehrungsnetzes auf den Schubwiderstand und das Bruchverhalten aufzuklären. Es wird klar, dass dies einer der hauptsächlichsten Gründe für den schweren Schaden bei Stahlbetongebäuden ist, wenn diese der Zähigkeit ermangeln. (Fig. 1 und 2)

Vc

DISCUSSION LIBRE / FREIE DISKUSSION / FREE DISCUSSION

The Impact Resistance of Prestressed Concrete

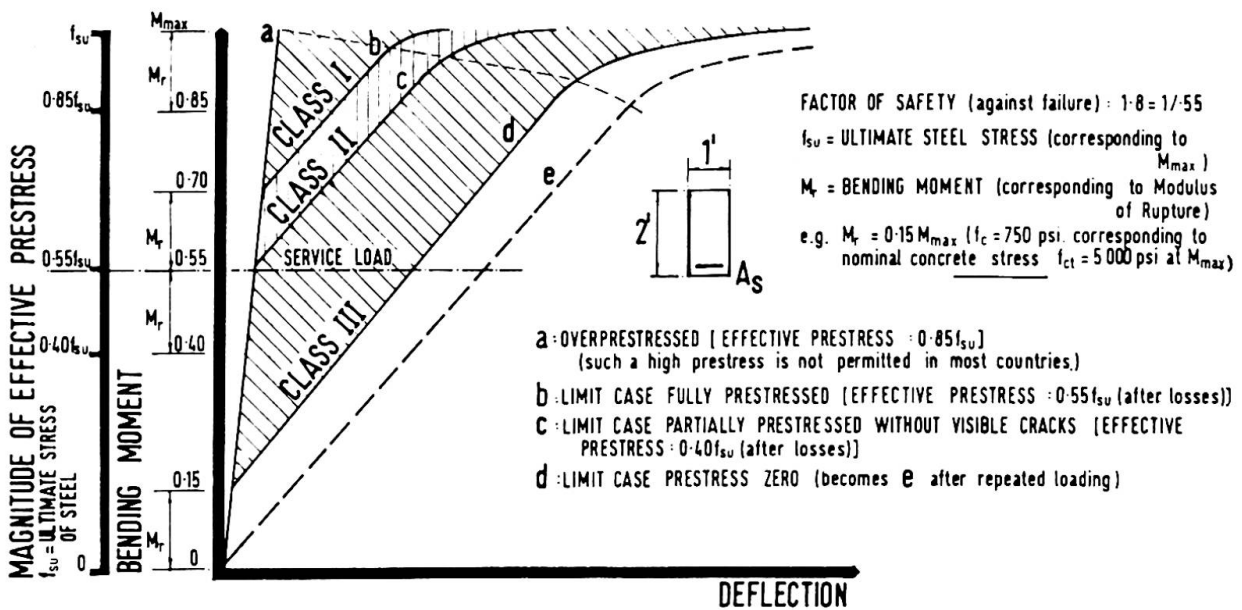
Résistance aux chocs du béton précontraint

Der Stoßwiderstand des vorgespannten Betons

P.W. ABELES

The contribution by Professors Newmark and Hall shows clearly the ductility of under-reinforced concrete members. It is remarkable that even without a favourable compressive reinforcement "the removal and re-application of load had little or no effect on either the load carrying capacity or the ultimate ductility". The title of the paper covers the "dynamic behavior of reinforced and prestressed concrete". Mr. Rogers in his contribution stated that prestressed concrete should not be used for earthquake frame structures. However, I should like to point out that the conditions with prestressed concrete may vary to a great extent dependent on the degree of prestress. In the figure below comparative bending moment deflection curves of under-reinforced rectangular prestressed concrete beams are shown in which all steel members are tensioned. Curve (a) presents a case at which cracking and failure occur simultaneously. This would be only obtained if the steel were over-prestressed and an effective prestress of 85% of the maximum were available which is not permitted in most countries. However, type (b) shows the limit case of fully prestressed concrete at which under service load which is supposed to be 55% of the failure load no tensile stresses occur. Curve (c) refers to a partially prestressed construction Class II of FIP-CEB at which the effective prestress is 40% of the maximum steel stress and under service load the first cracks just become visible, whereas type (d) relates to the limit case at which the effective prestress is zero. After repeated loading this case may become identical with type (e). It is seen that the ductility is greatly increased by reduction of the effective prestress. In the diagram the classification of FIP-CEB I, II and III is indicated.

COMPARATIVE BENDING MOMENT - DEFLECTION CURVES OF UNDER-REINFORCED RECTANGULAR PRESTRESSED CONCRETE BEAMS [ALL STEEL MEMBERS TENSIONED]



The ductility of prestressed concrete is essential where impact has to be absorbed. This has been demonstrated by impact tests on partially prestressed poles which I had shown at the Lisbon Congress twelve years ago. Reference is made to Figs. 5-7 in publication (1), the first shows the impact when a wagon of 45 kips weight was propagated with a speed of 10 miles per hour into a pole and cut off part of the flange. The pole was still capable of carrying the design load in spite of some wires in the flange being cut off. This demonstrates the ductility to impact.

- (1) Impact Resistance of Prestressed Concrete Masts" by P. W. Abeles, 17th Volume of Publications of IABSE (originally presented at Lisbon Congress at theme (b))